Sakarya University Journal of Science

ISSN : 2147-835X
Publisher : Sakarya University

Vol. 28, No. 3, 668-684, 2024
DOI: https://doi.org/10.16984/saufenbilder.1408939

Research Article

Investigation of Modifying Alloying Elements in High-Pressure Injection Casting Eutectic Al-Si Alloys

Alparslan Kılıçarslan[1*], Hatem Akbulut[2]

[1] Ayhan Metal Pressure Casting A.S., Kocaeli, Türkiye, alpaslankilicarslan@gmail.com
[2] Sakarya University, Faculty of Engineering, Department of Mettallurgy and Materials Engineering, Sakarya, Türkiye
[2]NESSTEC Energy & Surface Teknologies A.S., Tecnology Development Zones, Sakarya, Türkiye, akbulut@sakarya.edu.tr
[*]Corresponding Author

ARTICLE INFO

Keywords:
AlSi12(Fe) alloy
High-Pressure casting
Ti and Sr modification
Microstructure
Mechanical properties

Article History:
Received: 23.12.2023
Accepted: 13.05.2024
Online Available: 24.06.2024

ABSTRACT

In the study, the mechanical properties of aluminum alloys produced by the injection molding method, especially using Strontium and Titanium metals, were optimized without being subjected to cold forming. Mechanical tests were applied to the alloys produced by the high-pressure casting technique, and their strength, hardness, and microstructure were examined. Optical and SEM microscopy examinations investigated grain structures. Within the scope of the study, AlTi5B1 master alloy and AlSr10 master alloy were added to the pure AlSi10 (Fe) alloy in 5 different compositions. AlTi5B1 master alloy added to pure AlSi10(Fe) alloy significantly increased the hardness by reducing the grain size. Si modification took place with the addition of AlSr10 master alloy, and it was observed that the obtained weight ratios of 150ppm, 300ppm, and 450ppm Sr increased the hardness proportionally by 2.5 HB each. With the increase in Ti and Sr master alloys added, a significant increase was observed in tensile and yield strengths and % elongation rates. In the compression test, the percentage (%) deformation elongation, the reduction of the grain structure of the material by the added Ti and Sr elements, and the transformation of the eutectic silicon into a spherical structure absorbed the applied Fm force. This led to an increase in strength, and while the permanent deformation elongation decreased as the weight of Ti increased, it was observed that the permanent deformation elongation decreased proportionally with each added amount of 150 ppm Sr. The addition of the Ti element reduced the grain size by shrinking the α-Al dendrites, but it did not affect the eutectic Si.

1. Introduction

Ti and Sr elements are widely used as grain refiners and modifiers in aluminum alloys to increase the durability of the material by improving its mechanical properties. In aluminum alloys, the strength is increased by low-temperature pressing (dislocation formation) to obtain the required strength under a certain load. The structure after the deformation process applied to Al and its alloy in the rolling manufacturing method elongation of equiaxed grains in the direction of rolling and with the elongation allowing shape change within the structure in direct proportion to the refinement of the force. The strengthening of the material occurs as a result of the increase in the number of dislocations at the grain boundaries. It restricts and creates stress hardening within the structure. With stress hardening, An increase in the strength properties of the material is observed [1].

It has been expected that the mechanical properties of aluminum alloys produced by injection molding, especially those using Sr and Ti metals, will be improved without the need for cold forming. A unique aluminum alloy with

Cite as: A. Kılıçarslan, Akbulut H. (2024). Investigation of Modifying Alloying Elements in High-Pressure Injection Casting Eutectic Al-Si Alloys, *Sakarya University Journal of Science*, 28(3), 668-684. https://doi.org/10.16984/saufenbilder.1408939

high strength and low permanent deformation was developed by adding some alloying elements to aluminum alloys in different proportions as grain refiners and modifiers. To improve the formability, roduction efficiency, and mechanical propertiesf Al-Mg-Si alloy, 6063 aluminum alloy. It has been found that melting the homogeneous billet in the second stage and cooling it in the furnace not only produced brittle cracks during the extrusion process but also refined the grain size. Online quenching of 6063 aluminum alloy profiles with complex cross-sections can prevent abnormal grain growth during the offline solid solution process and improve production efficiency. The strength of profiles extruded from cast billets and air-cooled homogeneous billets was found to be comparable. Therefore, most 6063 aluminum alloy profiles are extruded directly from molten billets without the need for homogenization, improving production efficiency. It was found that homogeneous billets cooled in the furnace had the lowest flow stress. This shows that the breaking force that can cause extrusion is lower. It is recommended to use oven-cooled homogeneous blanks for profiles with complex cross-sections or requiring high performance. In the Al-Mg-Si AA 6068 alloy, including Cu and Zr, microstructure, mechanical properties, and fatigue properties were studied. The alloy was characterized in its original form after homogenization, extrusion, and T6 heating. The microstructure and fracture morphology of the fractured samples were analyzed using optical microscopy, scanning electron microscopy, transmission electron microscopy, and energy dispersive spectrometry. The quasi-static strength of the AA 6086 aluminum alloy was significantly higher than some other AA 6xxx alloys, but the ductility remains almost the same. Extensive fatigue test results under low-cycle fatigue (LCF) and high-cycle fatigue (HCF) conditions demonstrated good fatigue resistance. The new AA 6086 aluminum alloy has provided a reasonable basis for engineering design applications [2].

Controlling the microstructure and mechanical properties with additively produced aluminum-silicon alloys has been reported to be an important part of the automotive and aerospace industries. This is a popular choice that has proven to be cost-effective, with good defect tolerance and static properties. However, these alloys have unique properties when processed via laser powder bed fusion (LPBF). Although finely dispersed silicon precipitates can produce fine-grained microstructures with superior static properties than their cast counterparts, they cause weak directional connections through layered deposition. This reduces shear and crack resistance, weakening and strengthening the structure. Therefore, these effects must be taken into account in the design of parts produced using LPBF. Heat treatments can complement machining procedures and improve critical properties such as ductility and fatigue strength, but often reduce the static strength of the material. In general, a more comprehensive range of achievable properties, including tensile, compressive, and torsional behavior, fracture toughness, and fatigue resistance, are achieved [3]. The nanostructured Al-9%Si-3%Cu alloy obtained by direct metal laser sintering (DMLS) was then processed using the high-pressure torsion (HPT) process. This results in significant grain refinement down to 60 nm, as well as significant dislocation density. These results demonstrate that controllable ultra-fine-grained microstructures can be achieved through coating fabrication and efficient severe plastic deformation processes [4].

Controlling microstructure and, therefore, mechanical and physical properties have been widely used for aluminum alloys, including age hardenable alıminum alloy materials [5]. In general, the researchers demonstrated that grain refinement can not only refine the grain size but also achieve partially modified microstructure from coarse silicon particles broken up into smaller pieces [6].

Since the excellent casting behavior and mechanical and corrosion properties of Al-Si-based alloys for the manufacture of lightweight components with complex geometries, grain refinement to improve the properties further needs to use different alloying elements and modifiers. The addition of Sr and Ti alone as solutes has little effect on grain size. Because of this, together with the Sr addition to the Al-Si

alloys, Ti addition is also aimed at using the Al-5Ti-1B refiner [7]. It has been reported by Bogdanoff et al., that the addition of 0.12–0.13% Ti and 100–150 ppm Sr modification elements into the Al-Si alloys results in a continuous increase of Si content with an apparent strength increase up to an amount of 11.4% [8]. It has been reported that the combined addition of Ti and Sr resulted in a considerable improvement in tensile properties for the extruded and T6-heat-treated Al 6070 alloys [9].

In the Al-Si-Cu-Ni alloy, Dong et al. found that the combined effect of Ti and Sr on the microstructure and mechanical properties of the alloy was positive. They have shown that the addition of 0.1% Ti and 0.02% Sr significantly reduced grain size and changed the morphology of eutectic Si. The strength and plasticity were increased considerably with ultimate tensile strength, yield strength, and elongation [10]. Similarly, Lee et al. studied the effect of Sr modifier and Ti in the form of an Al-Ti-B grain refiner in the Al-7Si-0.35Mg cast alloy, and they investigated the interaction between Sr and Al-5Ti-1B. They reported that the combined additions of Sr and Ti produced both eutectic Si modification and α-Al grain refinement while increasing the nucleation frequency of Al-Si eutectic grains compared to an alloy with the addition of Sr alone [11].

In this study, in the commercial AlSi12 alloy, the systematic research on the microstructural and mechanical properties is aimed to perform. The double addition effect of Ti and Sr on the primary a-grain and eutectic silicon crystals is targeted to optimize.

2. Experımental Studies

2.1. Method

Within the scope of this study, the modification of aluminum and silicon was achieved by adding Ti and Sr to the AlSi12 (Fe) alloy cast under high pressure. At the same time, the addition of Ti modified Al, the addition of Sr modified Si. Ti addition affects grain refinement. The mechanical effects of Ti addition and Sr addition on the eutectic Si alloy were investigated. To examine the impact of Ti modification and Sr modification on Al-Si alloy parts produced by the high-pressure casting method, Sr alloys were tried at 0.08% Ti and 0 ppm (without Sr addition), 150ppm, 300ppm, and 450ppm rates. A Radiographic (Digital RT) examination of the parts produced in the casting was carried out. The method applied in the experimental study, and the alloys used are shown in Figure 1.

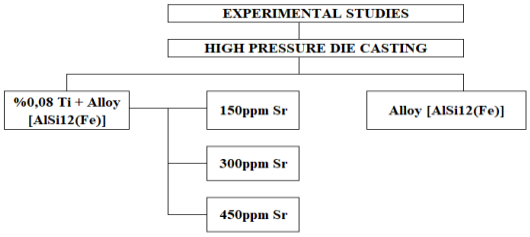

Figure 1. Methods and alloys applied in the experimental study schematic (representation)

Casting was made from AlSi10(Fe) ingot in accordance with EN AC 44300 standard, without adding Ti and Sr to pure AlSi10(Fe). Casting was carried out by adding AlTi5B1 master alloy with 0.08% Ti alloy by weight. Casting parts were produced by adding AlSr10 master alloy for 150ppm Sr, 300ppm Sr, and 450ppm Sr alloys by weight. A total of 20 prints were obtained from a single charge in approximately 30 minutes, with a cycle time of 90 sec/print. The tests carried out within the scope of the experimental studies applied to the obtained sprue parts are shown in Figure 2.

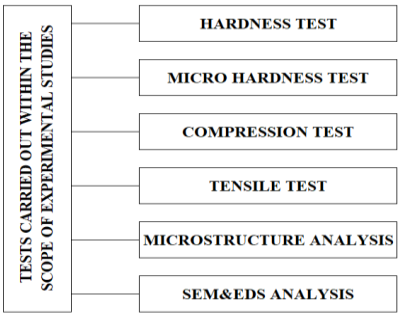

Figure 2. Tests to be applied in experimental studies schematic (representation)

2.2. Alloys and materials used in the research

AlSi12(Fe) alloy was used in the experimental study. The alloy's equivalent in international standards is EN AC 44300 (EN), ISO AlSi12(Fe) (DIN EN 1676), ETİAL140 (Eti Alüminyum), LM6(UK), A-S13(FR), UNI 4514, AC3A(JPN).

and in AA, it is known as ASTM-A413(USA). For pure AlSi10(Fe), the percentage (%) chemical composition of the alloy without adding Ti and Sr is given in Table 1.

Table 1. Percentage of chemical composition of pure AlSi12(Fe) alloy used in experimental studies

Si%	**Fe %**	**Cu %**	**Mn %**	**Mg%**	**Cr %**	**Zn %**
Avr. 12,0842	0.81	0.0857	0.0927	0.2879	0.0142	0.0804
Min. 10,5	0.45	0	0	-	-	0
Max. 13,5	1	0.1	0.55	-	-	0.15
Ni%	**B%**	**Be %**	**Co %**	**Ca%**	**Cd %**	**Pb %**
Avr. 0,0168	0.0044	<0.003	0.0065	0.0062	<0.001	0.0097
Min.	0	0	0	0	0	0
Max. 0.15	0.05	0.05	0.05	0.15	0.01	0.1
Sn%	**Ti%**	**V%**	**Sr%**	**Al%**		
Avr. 0,0047	0.0477	0.0147	0.002	86.4309		
Min. 0	0	0	0	0		
Max. 0.05	0.15	0.05	0.05	remainder		

2.3. Modification materials

AlTi5B1 master alloy was used for aluminum modification. AlTi5B1 master alloy was used in the form of bars with a diameter of 10 mm and a length of 500 mm. The percentage (%) chemical composition of the master alloy used in the experimental study is shown in Table 2.

Table 2. Weight % chemical composition of the AlTi5B1 master alloy used in the experimental study

Master Alloy	Al	Ti	B	Si	Fe	Mg
AlTi5B1	Remainder	5 1	1 1	<0.15	<0.20	<0.10

AlSr10 master alloy was used for silicon modification. AlSr10 master alloy was used in the form of rods with a diameter of 10 mm and a length of 750 mm. The percentage (%) chemical composition of the master alloy used in the experimental study is shown in Table 3.

Table 3. Weight percent chemical composition of the AlSr10 master alloy used in the experimental study

Master Alloy	Al	Sr	Fe	Si	Ca	Mg
AlSr10	Remainder	9-11	<0.30	<0.30	<0.10	<0.10

2.4. Hardness test

12mmx12mm analysis sample pieces were taken from 5 different samples. Each sample piece was sanded using papers of 240, 400, 800, 1000, and 1200 grid degrees, respectively. 10 measurements were taken from each sample by applying a load of 62.5 kg. The results obtained were calculated by subtracting the lowest and highest values and taking their average.

2.5. Microhardness test

Microhardness tests were conducted, and measurements were made on a-Al matrix and eutectic silicon. 10 measurements were taken from each sample. During the microhardness test process, a load of 25 kg was reached in 10 seconds. The results obtained were calculated by subtracting the lowest and highest values and taking their average.

2.6. Tensile test

Tensile tests for cylindrical tensile bars obtained from 5 different alloy samples were carried out according to ISO 6892-1 standard. The pulling speed is set as a standard of 1 mm/ min. To calculate the actual percentage (%) extension, an extensometer was used in the 25mm-40mm size range. Preload is applied as 5kg and 0.5mm/ min. 5 tensile tests were performed for each parameter. In the analysis, tensile strength, yield strength, and percentage (%) elongation values of the samples were taken.

2.7. Compression test

Non-runner samples obtained from 5 different samples were carried out according to BIS 452 and ISO 7500-1 annex 1 standard. The standard pressing speed was 2 mm/min. An extensometer with a 25mm-40mm range was used to calculate the actual percentage (%) of Deformation Elongation.

The application was made at max FP, and the preloading application was completed at FM(1/2FP). After removing the FP load, the compression process was reversed, and the difference in deformation in FM was calculated. The samples are placed between two plates with a strength of 65 HRC. It is subject to a preload of 65 kN (half the load to be applied). The load was increased to 130 kN. Development of % deformation: It is calculated as the change between the first applied 65kN load and the last applied 65kN load. For each alloy, 5 compression tests were performed, and the average was taken.

2.8. Microstructure analysis

12mmX12mm analysis sample pieces were taken from 5 different samples. Each sample piece was sanded using 240, 400, 800, 1000, and 1200 grid-grade papers, respectively. Samples are dried after filing intervals to prevent oxidation. Then, the samples were polished. Colloidal silica baize (iron-free polishing material) was used in the polishing process. After polishing, images were taken and subjected to engraving. After cauterization, optical images were viewed. Etching was done by preparing Keller's solution. The Keller Composition Table is given in 4 Morphological structures, and grain sizes were examined in microstructural imaging.

Table 4. Composition of Keller's solution

Etchant	Composition
Keller Solution	Pure Water 190 ml Nitric Acid (conc .) 5 ml Hydrochloric Acid (conc .) 10 ml Hydrofluoric Acid (48%) 2ml

2.9. SEM & EDS analysis

Microstructure of the samples after Ti and Sr modification were analyzed at ×1000 magnification. A Backscatter electron detector (BSED) was used in the SEM analysis. From the images obtained, Point and regional EDS analysis graphs and visuals were created. Percentage (%) of chemical combinations were obtained from the graphs. Intermetallic phases were examined in SEM image and EDS analysis.

3. Results and Discussion

3.1. Hardness test results

The test was prepared by cross-sectioning 5 different alloy pieces, each cast in different compositions. The average hardness values of the samples are given in Table 3. It was observed that the hardness value of pure AlSi10(Fe) increased by 5 HB by increasing the Ti ratio to 0.08%. A significant increase in the hardness value of the alloys was observed with every 150ppm Sr increase added while keeping the Ti ratio at 0.08%. The alloy with the highest hardness is AlSi10(Fe) alloy containing 450ppm Sr.

Table 5. Average Brinell hardness values

Alloys	Hardness Value (HB)
Alloy [AlSi12(Fe)]	65,3
Alloy + %0.08 Ti	70
Alloy + %0.08 Ti + 150ppm Sr	72.7
Alloy + %0.08 Ti + 300ppm Sr	74.8
Alloy + %0.08 Ti + 450ppm Sr	77.3

In high-pressure casting, the hardness of the AlSi12(Fe) alloy with a 0.08% Ti ratio increased with the addition of Sr after the grain refinement increased. The increase in hardness value increased proportionally with the addition rate. It was observed that the hardness of the 150ppm Sr added AlSi10(Fe) alloy increased by 2.5 HB, with 300ppm Sr increase, the hardness of the added AlSi10(Fe) alloy increased by 5 HB, and the hardness of the 450ppm Sr added AlSi10(Fe) alloy increased by 7.5 HB. The curve and standard deviation in hardness changes are shown in Figure 3.

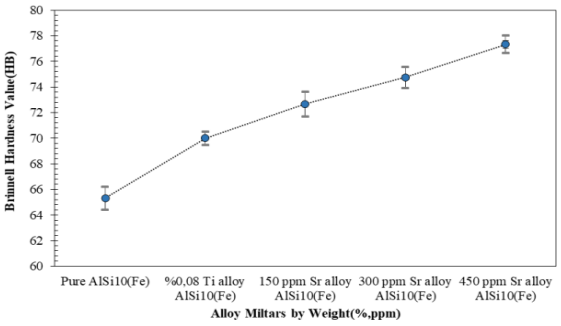

Figure 3. Alloys with 5 different weight compositions, standard deviation, and average hardness values obtained depending on additions.

3.2. Microhardness results

The average microhardness values of α-Al dendrite and eutectic silicon phases formed after Ti and Sr modification are given in Table 5. In α-Al Dendrite microhardness values, the microhardness value showed a significant increase by increasing the Ti ratio to 0.08% in the pure AlSi10 (Fe) alloy. It was observed that the microhardness value of the alloys continued to increase significantly with each 150ppm Sr increase while keeping the Ti ratio at 0.08%. In Eutectic Silicon microhardness values, the microhardness value did not show a significant increase by increasing the Ti ratio to 0.08% in the pure AlSi10 (Fe) alloy. It was observed that the microhardness value of the alloys continued to increase significantly with each 150ppm Sr increase while keeping the Ti ratio at 0.08%, are shown in Table 6.

Table 6. Average Vickers microhardness values

Alloys	α-Al Dendrit (HV/25/10)	Eutectic Silicon (HV/25/10)
Alloy [AlSi12(Fe)]	77	113
Alloy + %0.08 Ti	109	117
Alloy + %0.08 Ti + 150ppm Sr	138	162
Alloy + %0.08 Ti + 300ppm Sr	175	198
Alloy + %0.08 Ti + 450ppm Sr	216	256

In α-Al Dendrite microhardness values, after the significant increase in the microhardness of the AlSi12 (Fe) alloy with 0.08% Ti content due to grain refinement, the increase with each 150ppm Sr addition was observed to be approximately 35 HV. When we look at the microhardness of Eutectic Silicon, it is seen that the addition of Ti does not have a significant effect on the hardness of Silicon. Still, the increase in microhardness as a result of Si modification with the addition of Sr increases by approximately 40 HV for each 150ppm increase. The curves of the changes in α-Al Dendrite microhardness are shown in Figure 4. The curves of the changes in eutectic Silicon microhardness and standard deviation are shown in Figure 5.

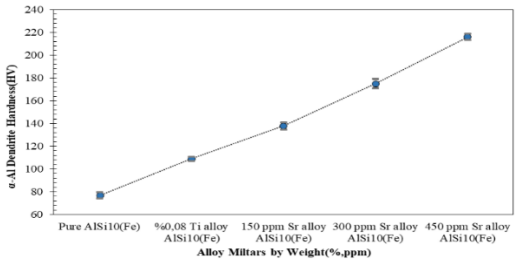

Figure 4. Alloys with 5 different weight compositions standard deviation and α-Al dendrite microhardness values obtained depending on additions.

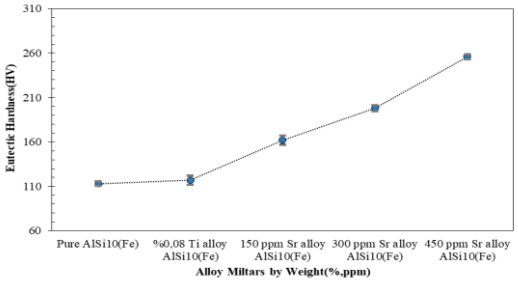

Figure 5. Alloys with 5 different weight compositions, standard deviations, and eutectic silicon microhardness values obtained depending on additions.

3.3. Tensile test results

The tensile strength (σ_t) values obtained from the tensile test results performed on 5 different alloy parts, each cast with different compositions, are shown in Table 7.

Table 7. Tensile strength values

Alloy by Weight	Tensile Strength σ_t (N/mm^2)
Pure AlSi10(Fe)	123
%0,08 Ti alloy AlSi10(Fe)	138
150 ppm Sr alloy AlSi10(Fe)	148
300 ppm Sr alloy AlSi10(Fe)	155
450 ppm Sr alloy AlSi10(Fe)	161

By increasing the Ti ratio to 0.08% in the pure AlSi10(Fe) alloy, a 15 MPa increase in tensile strength was observed. An increase of approximately 10 MPa in the tensile strength value of the alloy was contributed with a rise of 150 ppm Sr while keeping the Ti ratio at 0.08%. A 7 MPa increment was observed in the tensile strength value of the alloy with an increase of 300 ppm Sr and a 6 MPa increase in the tensile strength value of the alloy was observed with an increase of 450 ppm Sr. The curves of tensile strength changes are given in Figure 6.

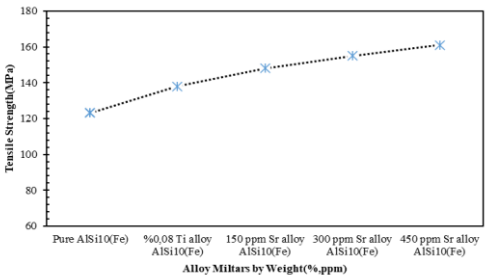

Figure 6. Tensile strength (σ_t) values obtained depending on alloys with 5 different weight compositions

Yield strength (σ_y) values obtained from the tensile test results are shown in Table 8.

Tablo 8. Yield Strength values

Alloy by Weight	Yield Strength σ_y (N/mm^2)
Pure AlSi10(Fe)	108
%0,08 Ti alloy AlSi10(Fe)	116
150 ppm Sr alloy AlSi10(Fe)	113
300 ppm Sr alloy AlSi10(Fe)	121
450 ppm Sr alloy AlSi10(Fe)	131

An 8 MPa increase in yield strength was observed by increasing the Ti ratio to 0.08% in the pure AlSi10(Fe) alloy. No significant increase in the yield strength of the alloy was observed with the rise of 150ppm Sr added while keeping the Ti ratio at 0.08%. Approximately 10 MPa increase in the yield strength value of the alloy was observed with the rise of 300ppm and 450ppm Sr. The curves of yield strength changes are given in Figure 7.

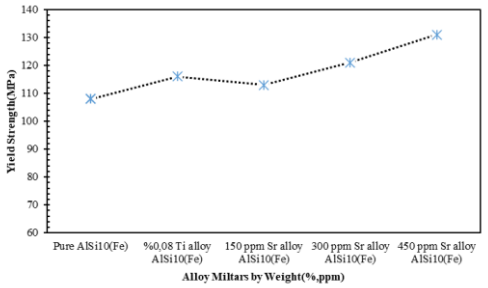

Figure 7. Alloys with 5 different weight compositions

Yield Strength (σ_t) values are obtained depending on the additions.

The percentage (%) elongation values obtained from the tensile test results are shown in Table 9.

Table 9. Percent (%) elongation values

Alloy by Weight	% Elongation
Pure AlSi10(Fe)	0.83
%0,08 Ti alloy AlSi10(Fe)	0.91
150 ppm Sr alloy AlSi10(Fe)	0.99
300 ppm Sr alloy AlSi10(Fe)	1.17
450 ppm Sr alloy AlSi10(Fe)	1.4

By increasing the Ti ratio to 0.08% in the pure AlSi10(Fe) alloy, a 0.08% increase in the percent (%) elongation value was observed. By keeping the Ti ratio at 0.08% and adding 150ppm Sr, the percentage (%) elongation value of the alloy is approximately 0.07%, with an increase of 300ppm Sr, the tensile strength value of the alloy is 0.18%, and with an increase of 450 ppm Sr, the alloy's percentage (%) elongation value is approximately 0.07%. An increase of 23 was observed. Curves of percentage (%) elongation changes are given in Figure 8.

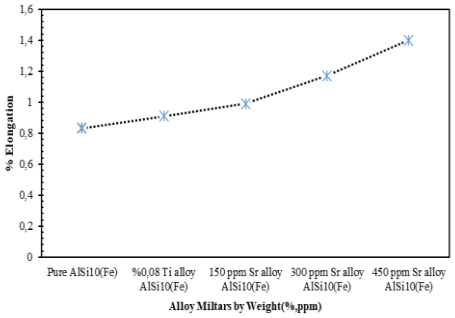

Figure 8. Percent elongation values obtained depending on alloys with 5 different compositions by weight

It has been found that the effect of Ti and Sr on the microstructure and mechanical properties of the Al-Si-Cu-Ni alloy is similar. It was observed that the addition of Sr and Ti together had a more distinct microstructure compared to the addition of Sr or Ti alone. They stated that the precipitates contained Al2Cu, Al3CuNi, and Al7Cu4Ni in the Al-12Si-4.5Cu-2Ni alloy. They concluded that strength and flexibility increased simultaneously with the combined effect of deposition defects and nano-Al2Cu, and the alloy transitioned from fracture to ductility. This result supports our study [12].

3.4. Compression test results

The permanent deformation values as % elongation under 130 kN load in the compression test performed for 5 different alloy parts, each

cast with different compositions, are shown in Table 10. A significant increase in the elongation was observed by increasing the Ti ratio to 0.08% in the pure AlSi10(Fe) alloy. Percentage elongation of the alloys with each 150ppm Sr increase added while keeping the Ti ratio at 0.08%. No significant increase was observed, but it was observed that it reduced permanent deformation by 1%.

Table 10. Average of % Deformation Elongation values as a result of compression test

Alloys	Deformation (% elongation) under 130 kN load
Alloy [AlSi12(Fe)]	0.335
Alloy + %0.08 Ti	0.282
Alloy + %0.08 Ti + 150ppm Sr	0.271
Alloy + %0.08 Ti + 300ppm Sr	0.265
Alloy + %0.08 Ti + 450ppm Sr	0.247

Permanent % deformation elongation values of compressive strength results are shown in Figure 9.

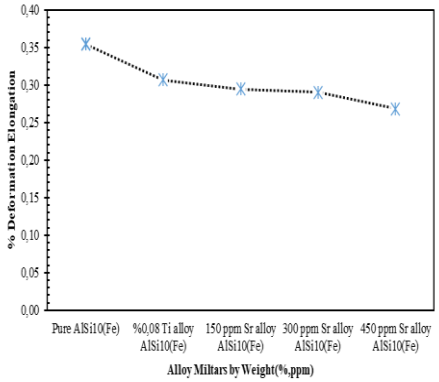

Figure 9. Average percent deformation elongation values obtained under 130 kN load depending on alloys with 5 different compositions by weight

3.5. Microstructure analysis results

It consists of 5 different alloy parts, each cast, polished, and engraved with a different composition. Optical microscopy results show that the microstructure image of α-Al dendrites and silicon eutectic phases formed after Ti and Sr modification during the growth process is shown in Figure 9. In a study investigating the microstructure and mechanical properties of phosphorus and Al-Ti-B on sub-eutectic silicon aluminum AlSi7Mg alloy, Ti/B was selected considering the optimal ratio of 5:1. Modifiers containing different contents of titanium, boron, and phosphorus were added to the AlTiBP master alloys; Phosphorus was added in amounts of 0.1%, 0.2%, and 0.3% by weight of the modified casting. The test results confirmed the modification effect of adding the parent alloy. Modifiers with different chemical compositions can achieve different microstructure morphologies. It was observed that the modifier containing 0.25% Ti + 0.03% B + 0.2% P had the most positive effect, and its measurable parameters (among the obtained parameters) had the highest mechanical properties. It was also concluded that titanium and boron affect the microstructure and mechanical properties of sub-eutectic silicon AlSi7Mg in the presence of phosphorus [13].

Microstructural images of pure AlSi10(Fe) samples are provided. When we examine the unmodified microstructure, it can be seen that the large eutectic silicon phase of α-Al dendrites is in the form of large plate-like and needle-like particles.

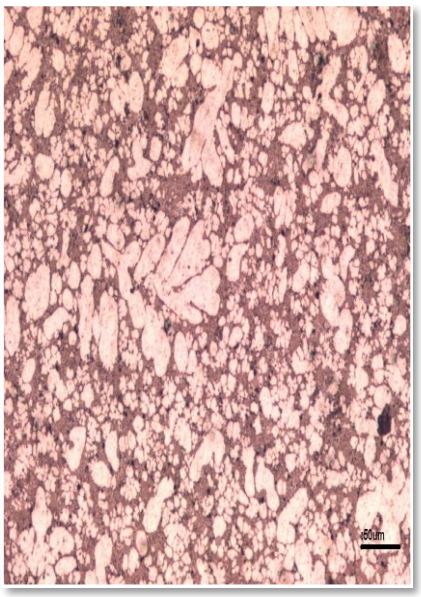

Figure 10. Microstructure images of pure AlSi10(Fe) sample

When we examined the microstructure images of the 0.08% Ti alloyed AlSi10(Fe) sample, it was observed that the α-Al dendrites became smaller. If the α-Al dendrites are in their state, they grow in the opposite direction of the heat, and long lateral arms are seen to increase. Since reducing the dendrites is the same as reducing the grain size, it has been observed that the grain size decreases. However, it was observed that the addition of Ti did not change the microstructure of eutectic Si Figure 10.

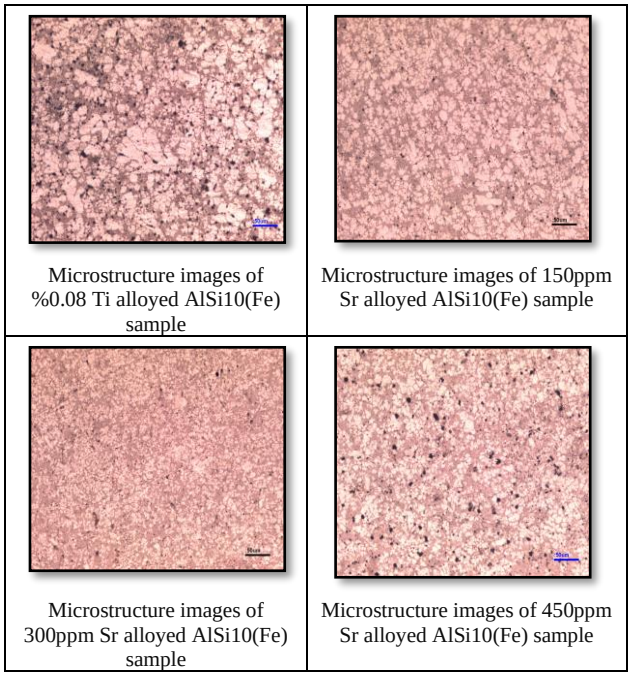

Figure 11. Microstructure of eutectic Si by Ti addition

When we examined the microstructure images of the 150ppm Sr alloyed AlSi10(Fe) sample, a needle-like structure in which large lamellae were fragmented in the eutectic silicon phase was observed. α-Al dendrites were small in size and tended to be spherical Figure 11.

It was observed that very little needle-like structure remained in the eutectic silicon phase. The α-Al dendrites reached a smaller size compared to the 150ppm Sr alloyed AlSi10(Fe) sample, and the spheroidization increased further.

When the microstructure images of the 450ppm Sr alloyed AlSi10(Fe) sample were examined, it was observed that the structure with the maximum increase in the eutectic silicon phase was fibrosis and spherical fibrous structure, as shown in.

In an A356 alloy, the addition of Ti and B significantly increases the toughness of the alloy, but only if the alloy is completely modified. Also, note that you must use the correct alloy type and addition amount. The highest total absorbed energy values recorded for tempered T6 alloys were obtained using Al–5%Ti–1%B and Al–10%Ti. There was an exception of 0.04% where impact properties were significantly degraded due to impact. It was concluded that the increase in strength can be attributed to Sr-B interactions (in some cases), changes in Si particle morphology, and dissolution and decomposition of some intermetallic compounds at T6 temperatures [14]. According to the morphology of silicon dioxide, the eutectic modification was upgraded and modified from the American Foundry Society (AFS) modification grade to AFS grade 5 [15].

The degradation degree of eutectic silicon according to silicon dioxide morphology is shown in Table 11. The degree of distortion, according to the American Foundry Association, is shown in Figure 12.

Table 11. Eutectic modification classification according to silica morphology

No	Classification	Silicon morphology
AFS 1	No modification	Large lamellar/acicular particles
AFS 2	Lamellar/acciform structure	Fine lamellar/acicular particles
AFS 3	Partial modification	Needle-like structure in which the lamellae are disintegrated
AFS 4	Reduced acicular structure	Structure in which tiny acicular phase remains
AFS 5	modified	Fibrosis/spheroidized structure

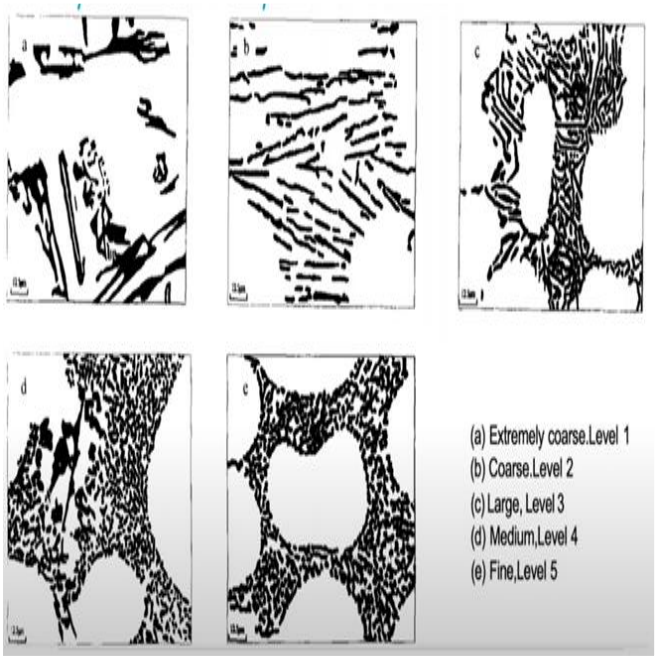

Figure 12. American Foundry Association modification levels [15]

Microstructure images of α-Al dendrite and eutectic silicon phases formed after Ti and Sr modification are shown in Figure 13.

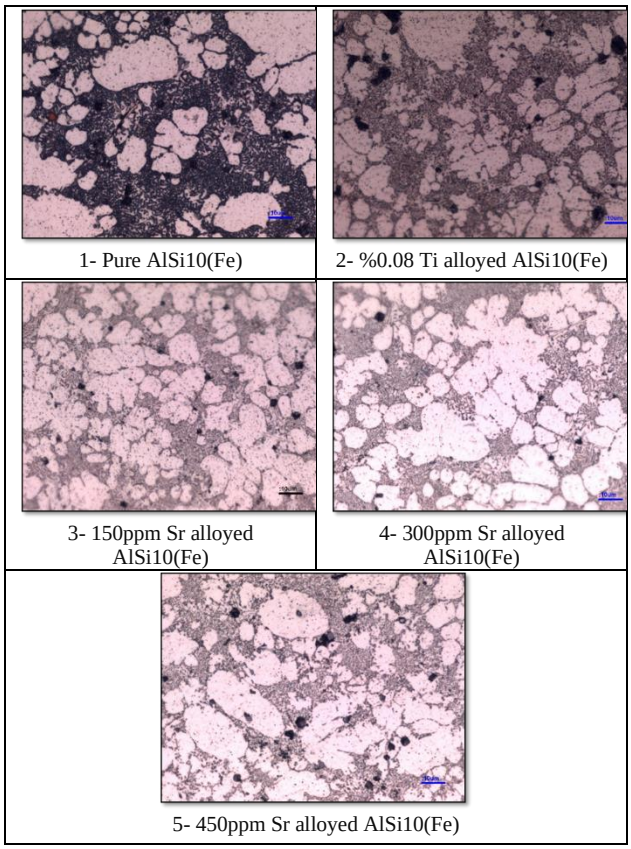

Figure 13. Microstructure images of samples obtained from alloys with 5 different weight compositions 1) Undoped AlSi10(Fe), 2) 0.08% Ti alloyed AlSi10(Fe), 3) 150ppm Sr alloyed AlSi10(Fe), 4) 300ppm Sr alloyed AlSi10(Fe) 5) 300ppm Sr alloyed AlSi10(Fe)

3.6. SEM analysis results

SEM images and EDS analyses were performed on the samples examined with an optical microscope. Microstructure images of α-Al dendrite and eutectic silicon phases formed after Ti and Sr modification are shown in Figure 14.

SEM images of the pure AlSi10(Fe) sample are given. When we examined the unmodified image, it was observed that the α-Al dendrites were very large, and the eutectic silicon phases were large lamellar and needle-like particles. However, no change was observed in the microstructure of eutectic Si.

In the literature study, high Fe-containing AlSi12 alloy was processed by laser powder bed fusion (LPBF) additive manufacturing to understand the properties of microstructures and mechanical properties in the fabricated state. Fe impurity was found to be beneficial for improving mechanical properties in LPBFed samples. Parameters including the combination of 200 W laser power, 1110 mm/s scanning speed, 0.15 mm cover gap, 0.03 mm layer thickness, and 40 J/mm3 laser volumetric energy density were optimized to achieve a high relative intensity of 99%. 7 As-LPBFed AlSi12FeMn alloy is found to have a high density, significantly refined spherical α-Al(Fe, Mn) Si phase (10-50 nm), consistent with the Al matrix. Meanwhile, the as-LPBFed AlSi12FeMn alloy can offer superior mechanical properties, including a yield strength of 305 MPa, ultimate tensile strength of 485 MPa, and fracture strain of 6.1%. The improved mechanical properties are attributed to synergistic strengthening mechanisms, including solid solution strengthening, grain boundary strengthening, and precipitation strengthening. Moreover, the formation of high-density deposition defects (SFs) and Lomer-Cottrell locks (LCs) in local regions has also resulted in the as-LPBFed AlSi12FeMn alloy, which can provide strengthening [16].

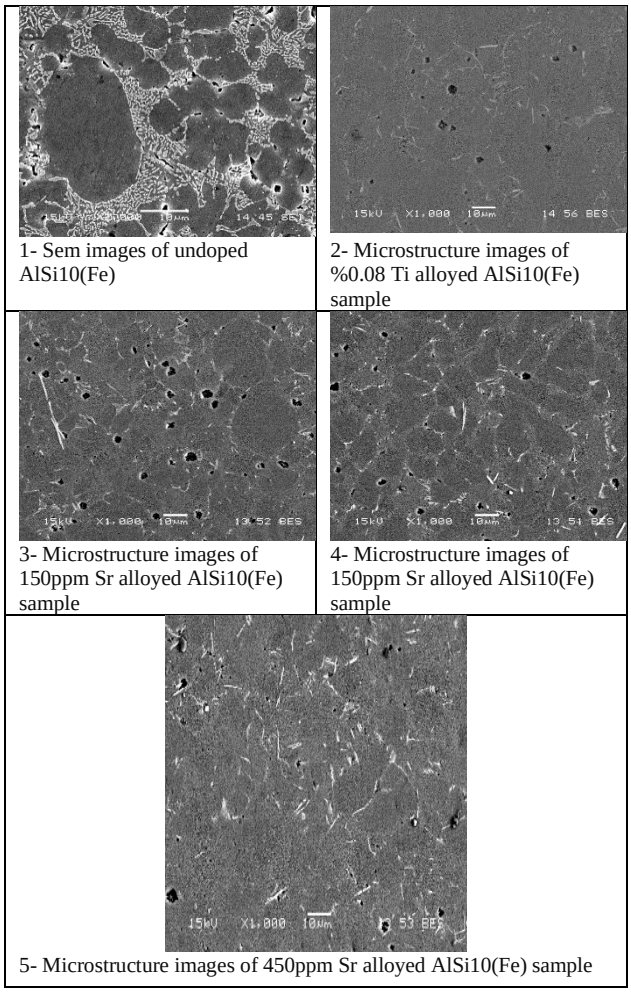

Figure 14. SEM images of samples obtained from alloys with 5 different weight compositions

1- SEM images of undoped AlSi10(Fe) sample, 2- Microstructure images of 0.08% Ti alloyed AlSi10(Fe) sample, 3- Microstructure images of 150ppm Sr alloyed AlSi10(Fe) sample, 4- Microstructure images of 300ppm Sr alloyed AlSi10(Fe) sample, 5- Microstructure images of 450ppm Sr alloyed AlSi10(Fe) sample.

When we examined the microstructure images of the 0.08% Ti alloyed AlSi10(Fe) sample, it was observed that the α-Al dendrites had become significantly smaller. For the microstructure images of the 150ppm Sr alloyed AlSi10(Fe) sample, it was observed that the large lamellae in the eutectic silicon crystals became smaller.
When the microstructure images of the 300ppm Sr alloyed AlSi10(Fe) sample were examined, more refined silicon was observed in the eutectic silicon crystals compared to the 150ppm Sr alloyed AlSi10(Fe) alloy. For the microstructure images of the 450ppm Sr alloyed AlSi10(Fe) sample, the most prominent thin silicones in the eutectic silicon crystals were observed. The black dots clearly observed in SEM images are residues from bakelite.

Point and regional EDS and analysis results of SEM images taken from pure AlSi10(Fe) alloy are given in Figure 15.

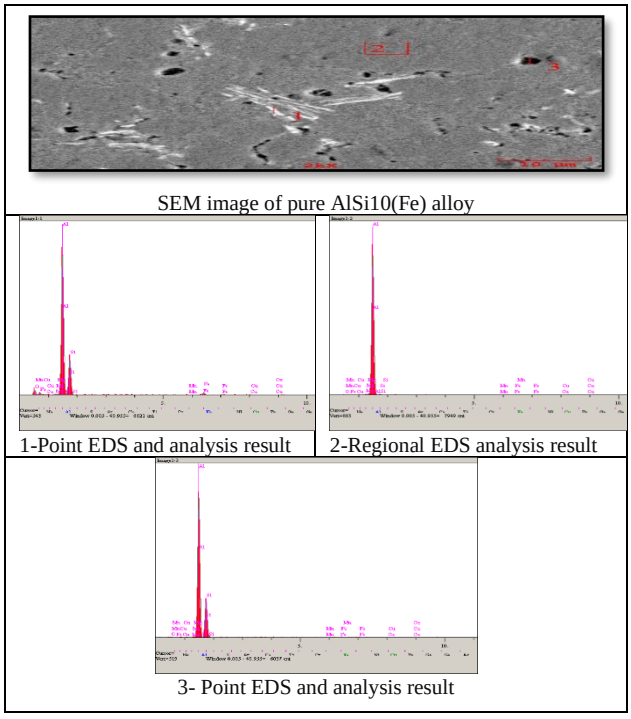

Figure 15. SEM image taken for the pure AlSi10(Fe) alloy sample and regional and point EDS analysis results obtained from this image

The chemical analysis compositions of the EDS results obtained are given below as point analysis, regional analysis, and point analysis results in Table 12.

Table 12. 1)Point analysis, 2)Regional analysis, 3)Point analysis, Results marked in the SEM image obtained for the pure AlSi10(Fe) alloy sample

Elt.	1. Point Analysis	2. Regional Analysis	3. Point Analysis	Units	
O	6.247	0.687	1.249	wt.%	
Mg	0.305	0.349	0.187	wt.%	
Al	60.133	96.132	64.177	wt.%	
Si	26.475	1.176	30.954	wt.%	
Mn	0.325	0.984	0.434	wt.%	
Fe	4.278	0.652	1.238	wt.%	
Cu	2.238	0.000	1.762	wt.%	
	100	100	100	wt%	Total

When we examined the EDS analyses, when we looked at the point analysis and regional analysis results, it was observed that the main components by weight of the elements in the intermetallic phases were Al, Si, Fe, Cu, O. There were trace amounts of Mg and Mn elements.

Point and regional EDS and analysis results of SEM images taken from 0.08% Ti alloyed AlSi10(Fe) alloy are given in Figure 16.

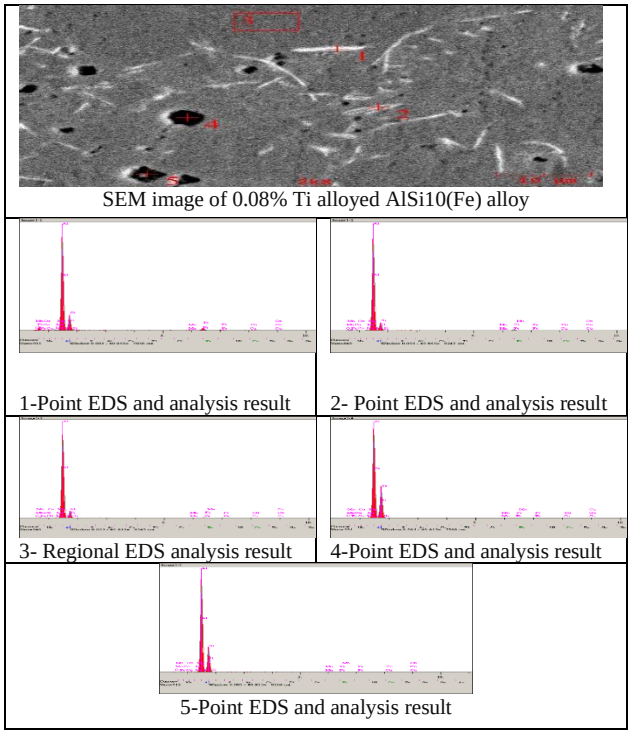

Figure 16. SEM image taken for the 0.08% Ti alloyed AlSi10(Fe) alloy sample and regional and point EDS analysis results obtained from this image.

The chemical analysis compositions of the EDS results obtained locally and regionally are given in Table 13.

Table 13. 1)Point analysis, 2)Point analysis, 3)Regional analysis, 4)Point analysis, 5)Point Analysis. Results marked in the SEM image obtained for the pure AlSi10(Fe) alloy sample

Elt.	1. Point Analysis	2. Point Analysis	2. Regional Analysis	4. Point Analysis	5. Point Analysis	Units
O	0.000	0.022	0.409	0.917	0.531	wt.%
Mg	0.516	0.369	0.120	0.206	0.060	wt.%
Al	69.352	82.022	96.139	60.756	66.865	wt.%
Si	18.712	12.555	1.148	34.770	31.691	wt.%
Mn	0.914	0.148	0.092	0.468	0.106	wt.%
Fe	8.388	3.559	0.730	1.347	0.692	wt.%
Cu	2.118	1.323	1.362	1.536	0.055	wt.%
	100	100	100	100	100	Total wt%

When we examine the EDS analyses, when we look at the point analysis and regional analysis results, it is observed that the main components by weight percent (%) of the elements in the intermetallic phases are Al, Si, Fe, and Cu. There are trace amounts of Mg, Mn, and O elements.
Point and regional EDS and analysis results of SEM images taken from 150ppm Sr alloyed AlSi10(Fe) alloy are given in Figure 17.

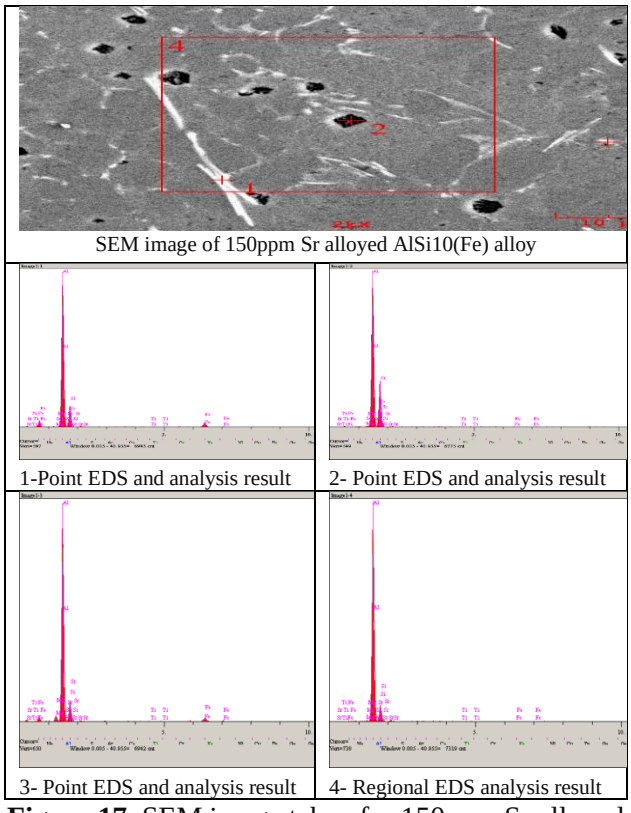

Figure 17. SEM image taken for 150ppm Sr alloyed AlSi10(Fe) alloy sample and regional and point EDS analysis results obtained from this image

The chemical analysis compositions of the EDS results obtained are given pointwise and regionally in Table 14.

Table 14. 1)Point analysis, 2)Point analysis, 3)Regional analysis, 4)Point analysis. Results marked in the SEM image obtained for the pure AlSi10(Fe) alloy sample

Elt.	1. Point Analysis	2. Point Analysis	3. Regional Analysis	4. Point Analysis	Units
Mg	0.183	0.193	2.064	0.380	wt.%
Al	71.198	64.567	74.768	84.407	wt.%
Si	17.053	33.181	13.890	13.869	wt.%
Ti	0.000	0.323	0.556	0.452	wt.%
Fe	11.566	1.019	8.722	0.892	wt.%
Sr	0.000	0.717	0.000	0.000	wt.%
	100	100	100	100	Total wt%

When we examined the EDS analyses, when we looked at the point analysis and regional analysis results, it was observed that the main components by weight of the elements in the intermetallic phases were Al, Si, and Fe. There were trace amounts of Mg, Ti, Sr elements. Point and regional EDS and analysis results of SEM images taken from 300ppm Sr alloyed AlSi10(Fe) alloy are given in Figure 18.

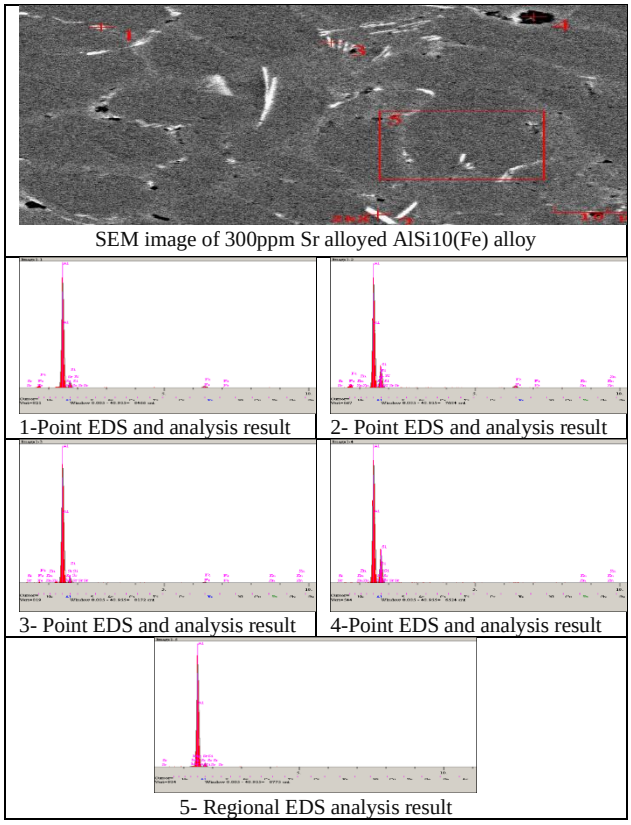

Figure 18. SEM image taken for 300ppm Sr alloyed AlSi10(Fe) alloy sample and regional and point EDS analysis results obtained from this image

The chemical analysis compositions of the EDS results obtained are given pointwise and regionally in Table 15.

Table 15. 1)Point analysis, 2)Point analysis, 3)Point analysis, 4)Regional analysis, 5)Regional analysis. Results marked in the SEM image obtained for the pure AlSi10(Fe) alloy sample

Elt.	1. Point Analysis	2. Point Analysis	2. Point Analysis	4. Regional Analysis	5. Regional Analysis	Units
Mg	-	-	-	-	0.488	wt.%
Al	82.322	67.313	84.776	67.142	92.514	wt.%
Si	9.108	21.771	8.202	30.580	6.998	wt.%
Fe	8.570	8.077	4.536	-	-	wt.%
Zn	-	2.838	2.486	0.685	-	wt.%
Sr	0.000	0.000	0.000	0.000	0.000	wt.%
	100	100	100	100	100	Total wt%

When we examined the EDS analyses, when we looked at the point analysis and regional analysis results, it was observed that the main components by weight percent (%) of the elements in the intermetallic phases were Al, Si, Fe, and Zn elements. Point and regional EDS and analysis results of SEM images taken from 450ppm Sr alloyed AlSi10(Fe) alloy are given in Figure 19.

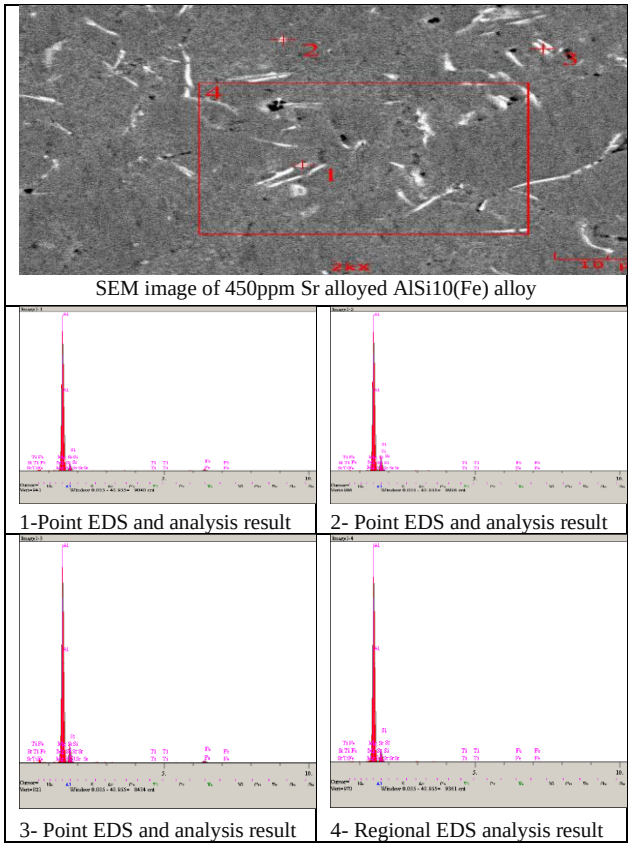

Figure 19. SEM image taken for the 450ppm Sr alloyed AlSi10(Fe) alloy sample and regional and point EDS analysis results obtained from this image

The chemical analysis compositions of the EDS results obtained as point and regional analysis are given in Table 16.

Table 16. 1)Point analysis, 2)Point analysis, 3)Point analysis, 4)Regional analysis. Results marked in the SEM image obtained for the pure AlSi10(Fe) alloy sample

Elt.	1. Point Analysis	2. Point Analysis	3. Point Analysis	4. Regional Analysis	Units
Mg	0.407	0.362	0.212	0.216	wt.%
Al	85.761	81.573	79.483	87.248	wt.%
Si	8.217	16.465	13.287	11.715	wt.%
Ti	0.306	0.183	0.330	0.132	wt.%
Fe	5.309	1.000	6.687	0.178	wt.%
Sr	0.000	0.416	0.000	0.511	wt.%
	100	100	100	100	Total wt%

When we examine the EDS analyses, when we look at the point analysis and regional analysis results, it is observed that the main components by weight percent (%) of the elements in the intermetallic phases are Al, Si, Fe, and there are trace amounts of Mg, Ti, Sr elements.

4. Conclusions and Discussion

4.1. Results

In this study, samples were produced by high-pressure casting method from alloys formed in 5 different compositions by adding Al5Ti1B master alloy and AlSr10 master alloy to pure AlSi10(Fe) alloy. The hardness, microhardness, mechanical properties, microstructure, and SEM analyses of the obtained alloys were examined comparatively.

1- In our study, the addition of Ti significantly increased the hardness by reducing the grain size. It is seen that the addition of 150ppm, 300ppm, and 450ppm Sr increases the hardness proportionally by 2.5 HB.

In the study, samples with different cross-sectional areas between 0° and 1° with an increment of 0.1° were produced from AA2024, AA6061, and AA7075 Al alloy sheets with a thickness of 2 mm by cutting them with the water jet method. The heat treatment process was applied to the test samples with different cross-sectional areas produced under two other

conditions. The first heat treatment process was used in the study. The heat treatment was applied by dissolving at 510°C for 2 hours + quenching + aging at 160°C. In the second heat treatment process, test samples were obtained by performing the heat treatment stages of 2 hours of dissolution at 510°C + quenching + 168 hours of shallow-cryogenic cooling at ≈ -75°C + aging at 160°C. At the end of each applied processing step, the hardness properties and natural frequency values of Al alloys were analyzed. When the hardness data of AA2024, AA6061, and AA7075 Al alloys were examined, it was determined that the applied heat treatment stages affected the hardness values of the materials. The supersaturated solid structure formed in the internal structure was obtained by quenching heat treatment after dissolving for 2 hours at 510°C applied to the Al alloy series, and it was determined that the time and temperature values during the used heat treatment stage were suitable for the AA2024, AA6061 and AA7075 Al alloy series. For the AA2024 Al alloy series, the maximum hardness value due to aging heat treatment was measured as 131HV after 7 hours. It was observed that the material hardness value started to decrease with the aging process continued after 7 hours. The maximum hardness value for AA6061 series Al alloy was measured as 93HV at the 12th hour. After this value was obtained, the aging process continued, and during the 13-15 hour aging process, it was observed that the hardness value decreased from 93HV to 74HV, and the aging process was completed for AA6061 Al alloy.

The data obtained in the hardness analysis taken after dissolution for AA7075 series Al alloy was measured as 31HV. The changes in the hardness properties of the material were examined with the aging heat treatment applied in 1-hour periods after the dissolution process. Accordingly, the maximum hardness value for the AA7075 Al alloy series was measured as 143HV at the 13th hour. After 13 hours, the aging heat treatment continued. Gradual decreases in hardness values were observed at 14 and 15 hours. 15. In the clock problem, the measured hardness value decreased from 143HV to 120HV [17].

2- In our study, Ti addition reduced the size of α-Al dendrites. The addition of Si changed the eutectic silicon phase. These two modified phases appear to increase the HV hardness significantly.

In the study, a new Al–11Si–3Cu alloy with high strength, flexibility, and low cost was developed by adding a small amount of Sr + Sc mixed substituent content. The effects of minor Sr and Sc contents on the microstructure and mechanical properties of the alloys were also investigated. In the study, a new high-strength, ductile, and low-cost Al-11Si-3Cu alloy micro-alloyed with little Sr + Sc was developed and shown to improve ultimate tensile strength and elongation over most developed Al-Si-3Cu alloys [18].

3- In our study, the addition of Ti and Sr elements showed a significant increase in tensile strength.
4- In our study, yield strength increased with the addition of Ti. Percentage (%) While there was no increase in 150 ppm Sr by weight, an increase was observed in 300 ppm and 450 ppm Sr.

In a different study, we investigated the effect of Ti and Sr addition on the microstructure and mechanical properties of Al-Si-Cu-Ni alloy and revealed the impact mechanism. The effect of Ti and Sr on the microstructure and mechanical properties of Al-Si-Cu-Ni alloy was investigated. Studies showed that the addition of 0.1% Ti and 0.02% Sr significantly reduced the grain size and changed the morphology of eutectic Si. Sr promoted the formation of stacking defects and nano-Al2Cu. The strength and plasticity increased significantly, with the ultimate tensile strength, yield strength, and elongation being 239.6 MPa, 140.6 MPa, and 2.11%, respectively. Our research showed that adding Sr and Ti together had a more distinct microstructure compared to adding Sr or Ti alone. The precipitates included Al2Cu, Al3CuNi and Al7Cu4Ni in the Al-12Si-4.5Cu-2Ni alloy. Strength and flexibility were simultaneously increased by the combined effect of stacking defects and nano-Al2Cu, and it was observed that the alloy transitioned from a brittle structure to a more ductile fracture [10].

5- In our study, a significant increase in % elongation values was observed with the addition of Ti and Sr.

In this thesis study, by making Sr modifications to the AlSi12(Fe) alloy produced using the high-pressure casting method, the effect of the amount of Sr on the mechanical and microstructural characteristics of the alloy was examined. As a result, it has been observed that both the microstructural and mechanical properties of the AlSi12 (Fe) alloy produced by the high-pressure casting method are positively affected depending on the increasing amount of Sr. A significant improvement was detected in the yield strength, tensile strength, and % elongation value of the AlSi12(Fe) alloy with increasing Sr amount. According to the results of the notch impact test, the energy absorption ability of the alloy was improved by increasing the amount of Sr. It was concluded that the ductility property of AlSi12(Fe) alloy was significantly enhanced with the use of 160 ppm Sr [19].

6- In our study, while the permanent deformation elongation decreased with the addition of Ti, it was observed that the permanent deformation elongation decreased proportionally with every additional 150 ppm Sr amount.

In the study, the effect of grain refinement (Al–5Ti–1B) and modification (Al–10Sr) on the microstructure, the morphology of the iron-containing needle-shaped beta phase, and the mechanical properties of the cast Al–12Si alloy were examined. Grain refinement of the alloy with the optimum amount of Al-Ti-B master alloy (0.00125 wt% Ti) in Al-12Si-based alloy reduces the size of Al-Fe-Si intermetallic compounds and transforms the needle-like β-morphology. Phase intermetallic compound into block form, similarly, modification of the alloy with the optimum amount of Al-Sr master alloys (0.06 wt% Sr) in the base metal Al-12Si alloy has been observed to refine eutectic Si [20].

7- In our study, it was observed that the addition of the Ti element reduced the grain size by shrinking the α-Al dendrites but did not affect the eutectic Si. It has been observed that the addition of the Sr element changes Si. When we reached 450ppm Sr, it was observed that it changed from a rough lamellar and needle-like structure to a fibrous/spherical structure.

8- In our study, it was determined that a-Al dendrites and Si crystals shrank in the images in SEM-EDS analyses, and this supports the optical image results. It has also been observed that there are intermetallic phases consisting of Al, Si, and Fe elements as the main components.

4.2. Suggestions

Based on the findings obtained as a result of experimental studies, the following suggestions can be made for future studies.

The effect of phosphorus on the same study can be investigated by using phosphorus along with strontium.

The effect of Ti and Sr over a certain period can be examined by taking samples from pressures at different times.

Except for the high-pressure casting method, the same experimental study can be carried out with the low-pressure casting method with the same parameters, and its effects on mechanical properties and microstructure can be examined.

Experiments can be made with different etchants to examine SEM images in detail.

Article Information Form

Funding
The author has not received any financial support for the research, authorship, or publication of this study.

Authors' Contribution
Alpaslan KILIÇARSLAN contributed conception / dizayn, data collection, data analysis/interpretation, writing, technical support / material support.

Prof.Dr. Hatem AKBULUT contributed data analysis/interpretation, technical support / material support, critical review of content, and literature review.

The Declaration of Conflict of Interest/ Common Interest
The authors have declared no conflict of interest or common interest.

The Declaration of Ethics Committee Approval
This study does not require an ethics committee permission or any special permission.

The Declaration of Research and Publication Ethics
The authors of the article declare they will respect the scientific, ethical, and rating rules of the SAUJS in all processes of the article and not carry out any falsification of the data collected. Furthermore, they state that the Sakarya University Journal of Science and its editorial board take no responsibility for any ethical violations that may be encountered and that this study has not been evaluated in any academic publishing environment other than the Sakarya University Journal of Science.

References

[1] X. Wang, G. Zhao, L. Sun, Y. Wang, H. Li, "A strategy to promote formability, production efficiency and mechanical properties of al–mg–si alloy," Journal of Materials Research and Technology, vol. 24, pp. 3853-3869, 2023.

[2] F. Zupanič, M. Steinacher, S. Žist, T. Bončina, "Microstructure, mechanical properties and fatigue behavior of a new high-strength aluminum alloy aa 6086", Contents lists available at ScienceDirect, Journal of Alloys and Compounds, vol. 941, pp. 168-976, 2023.

[3] J. Kadkhodapour, S. Schmauder, F. Sajadi, "Quality analysis of additively manufactured," Metals, Simulation Approaches, Processes, and Microstructure Properties, Chapter Nine, 1st Edition – November, vol. 30, pp. 886-9789, 2022.

[4] A. S. J. Al-Zubaydi, N. Gao, S. Wang, P. A. S. Reed, "Microstructural and hardness evolution of additively manufactured Al–Si–Cu alloy processed by highpressure torsion", Metals & Corrosion, Journal of Materials Science, vol. 57, pp. 8956–8977, 2022.

[5] O. Altuntaş, "Enhancement of impact toughness properties of Al 7075 alloy via double aging heat treatment", Gazi University Journal of Science Part C: Design and Technology, vol. 10, pp. 195-202, 2022.

[6] B. A. E. Haj, A. Hamadellah, A. Bouayad, C. E. Akili, "Review of grain refinement performance of aluminium cast alloys", Journal of Metallurgy and Materials Engineering, vol. 29-2, pp. 1-15, 2023.

[7] B. Callegari, T. N. Lima, R. S. Coelho, "The ınfluence of alloying elements on the microstructure and properties of al-si-based casting alloys: a review", Metals, vol. 13, pp. 1174, 2023.

[8] T. Bogdanoff, S. Seifeddine, A. K. Dahle, "The effect of si content on microstructure and mechanical properties of al-si alloy", Metall. Ital., vol. 108, pp. 65–68, 2016.

[9] M. Emamy, B. Pourbahari, M. Mostafapour, "Significant grain refinement and enhanced mechanical properties of 6070 Al alloy via Ti/Sr addition and hot extrusion", J. Ultrafine Grained Nanostruct Mater, vol. 53-2, pp. 190-203, 2020.

[10] J. Dong, J. Jiang, Y. Wang, M. Huang, Y. Liu, Y. Zhang, "Effect of Ti and Sr on the microstructure and mechanical properties of Al-12Si-4.5Cu-2Ni alloy", Materials Letters, vol. 352, pp. 135129, 2023.

[11] J. Y. Lee, J. M. Lee, K. S. Son, J. I. Jang, Y. H. Cho, "A study on the interaction between a Sr modifier and an Al-5Ti-1B grain refiner in an Al-7Si-0.35Mg casting alloy", Journal of Alloys and Compounds, vol. 938, pp. 168598, 2023.

[12] A. P. Hekimoğlu, M. Hacıosmanoğlu, M. Baki, "Effect of zinc additives at different rates on the structural, mechanical and

tribological properties of EN AC-48100 (Al-17Si-4Cu-Mg) alloy", Journal of the Faculty of Engineering and Architecture of Gazi University, vol. 35, pp. 1799-1814, 2020.

[13] B. Yalçın, R. Varol, "Determınatıon of wear performance and some mechanıcal propertıes of sıntered tıtanıum alloys", Journal of the Faculty of Engineering and Architecture of Gazi University, vol: 24, pp. 63-72, 2009.

[14] J. M. Yu, N. Wanderka, A. Rack, R. Daudin, E. Boller, H. Markötter, J. Banhart, "Influence of ımpurities, strontium addition and cooling rate on microstructure evolution in Al-10Si-0.3Fe casting alloys", Journal of Alloys and Compounds, vol. 766, pp. 818–827, 2018.

[15] Y. S. Lerner, N. R. Posinasetti, "Metal casting principles and techniques", Editor: American Foundry Society, pp. 274, 2013.

[16] A. M. Samuel, H. W. Doty, S. F. H. Valtierra, F. H. Samuel, "Effect of grain refining and sr-modification ınteractions on the ımpact toughness of Al–Si–Mg cast alloys", Materials and Design, vol. 56, pp. 264–273, 2014.

[17] R. Arslan, "Investigation of the effects of shallow-cryogenic and aging heat treatments applied to AA2024, AA6061, AA7075 Al alloys on microstructure, hardness and natural frequency properties", Pamukkale University, Institute of Science, Department of Metallurgical and Materials Engineering, pp. 1-110, 2023.

[18] Z. Shi, R. He, Y. Chen, H. Yan, H. Song, C. Luo, Q. Nie, Z. Hu, "Microstructural evolution and strengthening mechanisms of a novel Al–11Si–3Cu alloy microalloyed with minor contents of Sr and Sc", Contents lists available at ScienceDirect, Materials Science & Engineering A, Materials Science & Engineering A, vol. 853 pp. 143738, 2022.

[19] İ. Sapmaz, "Investigation of the effect of Sr additions in AlSi12(Fe) high pressure casting alloy on the microstructure and mechanical properties of the alloy", Bursa Technical University, Institute of Science and Technology, pp. 1-99, 2021.

[20] S. H. Rodríguez, R. E. Goytia-Reyes, D. K. Dwivedi, V. H. Baltazar-Hernández, H. Flores-Zúñiga, M. J. Pérez-López, "On influence of Ti and Sr on microstructure, mechanical properties and quality, index of cast eutectic Al–Si–Mg alloy", Contents lists available at ScienceDirect, Materials and Design, Materials and Design, vol. 32, pp. 1865–1871, 2011.